Desalination and Water Treatment
www.deswater.com

doi: 10.5004/dwt.2023.29125

281 (2023) 26–37
January

Modified hemispherical solar distillers using contiguous extended cylindrical iron bars corrugated absorber

A.E. Kabeel[a,b,*], Mohammed El Hadi Attia[c], Moataz M. Abdel-Aziz[d], Wael M. El-Maghlany[e], A.S. Abdullah[a,f], Mohamed Abdelgaied[a], Ravishankar Sathyamurthy[g], Sayed A. Ward[b,h]

[a]*Mechanical Power Engineering Department, Faculty of Engineering, Tanta University, Tanta, Egypt, emails: kabeel6@f-eng.tanta.edu.eg (A.E. Kabeel), a.abdullah@psau.edu.sa (A.S. Abdullah), mohamed_abdelgaied@f-eng.tanta.edu.eg (M. Abdelgaied)*
[b]*Mechanical Power Engineering Department, Faculty of Engineering, Delta University for Science and Technology, Gamasa, Egypt, email: drsayedw@yahoo.com*
[c]*Department of Physics, Faculty of Science, University of El Oued, 39000 El Oued, Algeria, email: attiameh@gmail.com*
[d]*Mechanical Power Engineering Department, Faculty of Engineering, Horus University, New Damietta, Egypt, email: dr.moataz86@yahoo.com*
[e]*Mechanical Engineering Department, Faculty of Engineering, Alexandria University, Egypt, email: elmaghlany@alexu.edu.eg*
[f]*Mechanical Engineering Department, College of Engineering, Prince Sattam bin Abdulaziz University, Saudi Arabia*
[g]*Department of Mechanical Engineering, King Fahd University of Petroleum and Minerals, Dhahran, Dammam, Saudi Arabia, email: raviannauniv23@gmail.com*
[h]*Electrical Engineering Department, Shobra Faculty of Engineering, Banha University*

Received 7 May 2022; Accepted 3 November 2022

ABSTRACT

The current experimentation work aims to enhance the hemispherical solar distiller's yield by employing contiguous extended cylindrical iron bars as energy storage corrugated absorbers. After installing the contiguous extended cylindrical iron bars, the absorber surface is similar to the semi-circular corrugated surface; the extended cylindrical iron bars represent sensible storage materials. To get the optimal diameter of contiguous extended cylindrical iron bars that achieve the highest performance, three hemispherical distillers were designed, fabricated, and tested in the same El Oued, Algeria weather conditions, namely; first is a conventional hemispherical distiller (CHD), and the second and third are hemispherical distillers that include contiguous extended cylindrical iron bars (HD-CECIB) at different diameters of (8, 10, 12, and 14 mm). The experiments were conducted in two scenarios; in the first scenario, contiguous extended cylindrical iron bars with diameters of 8 and 10 mm were installed in the second and third distillers (HD-CECIB8 and HD-CECIB10), respectively. In the second-test scenario, contiguous extended cylindrical iron bars with diameters of 12 and 14 mm were installed in the second and third distillers (HD-CECIB12 and HD-CECIB14), respectively. The results show that 14 mm represents the optimal diameter of contiguous extended cylindrical iron bars that achieve the highest performance. The cumulative yield of a reference CHD reached 4.8 L/m^2·d. In comparison, the utilization of contiguous extended cylindrical iron bars with 14 mm diameter (HD-CECIB14) improved the accumulative yield to 8.35 L/m^2·d with an improvement of 74% when compared to CHD. Also, the daily thermal efficiency of HD-CECIB14 reaches 70.3%, with an improvement of 72.3% compared to CHD. Furthermore, the economic feasibility illustrated that using contiguous extended cylindrical iron bars of 14 mm diameter is a very effective choice because it reduces the distillate water costs produced by 41.2% compared to CHD.

Keywords: Hemispherical solar distillers; Extended cylindrical iron bars; Corrugated absorber; Sensible storage materials; Optimal diameter; Solar energy

* Corresponding author.

1. Introduction

Water is the primary factor in ensuring the survival of life on the planet. Unfortunately, in most parts of the world, there is a severe shortage of fresh water, which stymies progress in many areas. As a result, providing fresh water is one of the top priorities for bridging the gap, as countries all over the world spend a lot of money and effort attempting to bridge their water deficits and provide the quantities of consumable water they require, whether for drinking, domestic, industrial, agricultural, or other purposes [1–5]. Solar water distillation is one of the most environmentally friendly desalination techniques, as it utilizes sunlight to generate the energy needed to run it [6–9]. Despite the abundance of free and clean solar energy, its disadvantage is its low consumption compared to other, more expensive desalination technologies [10–15]. Many studies and scientific publications have been released to improve the daily yield of solar stills.

Attia et al. [16] empirically conducted the performance of hemispherical solar distillation employing various concentrations of graphite in order to find the optimal concentration for improving hemispherical solar distillation yield. According to the findings, the 35 g/L graphite concentration resulted in the highest yield of a hemispherical solar distillation device. Attia et al. [17] used gravel of various sizes (4–16 mm) to determine the optimal gravel size for improving hemispheric solar distillation yield. Per the analyses, the black gravel size 16 mm achieved the highest yield of a hemispherical solar distillation device, with a 57.1% improvement compared to the reference distiller's results. Attia et al. [18] empirically verified the use of El Oued sand grains with different concentrations to get the best concentration to improve the hemispherical distillation performance. The results concluded that the 30% (30 g/L) sand grain concentration achieved the highest cumulative yield of the hemispherical distillation device, with an improvement rate of 52.1%. Attia et al. [19] investigated the effects of phosphate bags on solar still products at 1 and 2 cm depths in the water. When compared to the findings obtained by the reference distiller (3.8 L/m^2), the phosphate bags are the best suitable for improving the solar still yield, which was improved to 4.9 and 5.3 L/m^2·d at a water depth of 2 and 1 cm, respectively.

Attia et al. [20] investigated the impact of sandbags on solar still products in 1 cm of water. When compared to the reference distiller, the sandbags boosted the performance of the solar still by 34.57%. The impacts of marble pieces and sandstones as energy storage materials in solar distillate manufactured of fiber-reinforced plastic sheet products were investigated by Panchal et al. [21]. According to the findings, the marble and sandstone chunks increased the conventional solar still performance. The effects of gravel, polyethylene, and sand as absorbent materials in glass solar distillate products were investigated by Nasri et al. [22]. The results showed that when gravel and polyethylene were used instead of sand, the rate of output was 32.20% and 16.67% higher, respectively. Abdelgaied et al. [23] experimentally conducted the effects of different thicknesses (20, 30, and 40 mm) and densities (16, 20, and 30 kg/m^3) of the sponge layer on tubular distiller performance. The sponge layer (30 mm and 16 kg/m^3) had a higher rate of production of 59.2% compared to tubular solar stills with different thicknesses of the sponge layer (20 and 40 mm) and densities (20 and 30 kg/m^3).

Madhu et al. [24] conducted an influence of on box sand on the thermal behavior of solar still in an experiment. The maximum exergy efficiency with boxes was found to be 13.2%, which is lower than the standard solar still without boxes and sand inside the basin. Kabeel et al. [25] examined the effect of cement-coated red bricks on solar still's thermal performance. Compared to standard solar stills, the researchers discovered that the cement-coated red bricks had a 45% higher production rate.

Attia et al. [26] conducted experimental studies on fins set at 5 and 7 cm spacing and various lengths of 3, 2, and 1 cm on the performance of hemispherical solar stills at a water depth of 3 cm. The results showed that the 2 cm in length and 7 cm spacing is the best configuration, as it improves distiller yield by 56.73%. Balachandran et al. [27] studied experimentally how to enhance the yield of solar stills with eggshells as a sensible heat storage material. The researchers concluded that eggshells (2.46 L/m^2·d) had a better production rate than solar stills without eggshells (2.07 L/m^2·d). Abdelgaied et al. [28] improved the tubular distillation yield by employing the copper circular hollow fins and storage materials below the basin. Sathyamurthy et al. [29] conducted an impact of finned absorbers on distiller production. Kateshia and Lakhera [30] utilized the pin fins hybridization with paraffin wax to improve the solar distillation yield. Bataineh and Abbas [31] utilized the fins hybridization with internal reflectors to enhance solar distillation production.

Mohamed et al. [32] studied the influences of fine natural stones on the yield of the solar distiller. They conducted that the fine stone improved the yield by 33.37% compared to the reference unit. Kabeel et al. [33] empirically examined the influences of the utilization of composite storage materials (black gravel and paraffin wax) on the performance of solar distillers. They found that the yield improved by 37.55% by utilizing composite storage materials. Kabeel and El-Said [34] studied the behavior of a solar distiller incorporated with an HDH desalination unit. They concluded that the yield and GOR of this hybrid system reached 18.25 L/m^2 and 2.57, respectively. Kabeel et al. [35] studied the performance of a hybrid SS-HDH desalination plant incorporated with a flashing chamber. They conducted that the distillate cost for utilizing the hybrid system reduced from 9.74 to 8.6 $/m^3 compared to the separated systems. The HDH water desalination systems have also been integrated with desiccant air conditioners, aiming to recover thermal energy and use it to improve the performance of HDH desalination units [36–40]. Kabeel and El-Said [41] presented a comprehensive review of the utilization of energy storage systems to improve the productivity of solar distillation. Also, Abdelgaied et al. [42] theoretically conducted the behavior of the HDH desalination unit incorporated with a reverse osmosis desalination system powered by PVT panels.

The experimentation work in the present manuscript aims to improve hemispherical distiller yield by employing

contiguous extended cylindrical iron bars as energy storage corrugated absorbers. After installing the contiguous extended cylindrical iron bars, the absorber surface is similar to the semi-circular corrugated surface, and the extended cylindrical iron bars represent sensible storage materials. To get the optimal diameter of contiguous extended cylindrical iron bars, those achieve the highest performance of hemispherical solar distillers. The three hemispherical distillers were designed, fabricated, and tested under the same El Oued, Algeria weather conditions, namely; the first is a conventional hemispherical distiller (CHD) that represent the reference case, and the second and third are hemispherical distillers that include contiguous extended cylindrical iron bars (HD-CECIB) at different diameters of (8, 10, 12, and 14 mm). The experiments were conducted in two scenarios; in the first scenario, contiguous extended cylindrical iron bars with diameters of 8 and 10 mm were installed in the second and third distillers (HD-CECIB8 and HD-CECIB10), respectively. In the second-test scenario, contiguous extended cylindrical iron bars with diameters of 12 and 14 mm were installed in the second and third distillers (HD-CECIB12 and HD-CECIB14), respectively. In the two experimentation test scenarios, the performance of second and third distillers with different diameters of the contiguous extended cylindrical iron bars are compared with CHD under the same El Oued, Algeria weather conditions to get the optimal diameter of contiguous extended cylindrical iron bars that achieves a highest hemispherical solar distillers performance.

To illustrate the influences of employing contiguous extended cylindrical iron bars as energy storage corrugated absorbers on the performance of hemispherical distillers. This manuscript is organized as follows: the first section deals with the desalination problems and most previous studies, the second section deals with the description of the experimental setup, the third section deal with the results and discussions, and the fourth section deal with comparing the results of the current study with other previous studies, and the fifth section deals with economic evaluation, and the sixth section deals the most important conclusions.

2. Experimental set-up

2.1. Setup design and configuration

This experimental work aims to achieve the highest hemispherical solar distiller productivity. To achieve this, the contiguous extended cylindrical iron bars as energy storage corrugated absorber was installed in the basin of the hemispherical distiller. After installing the contiguous extended cylindrical iron bars, the absorber surface is similar to the semi-circular corrugated surface, and the extended cylindrical iron bars represent sensible storage materials. To get the optimal diameter of contiguous extended cylindrical iron bars, those achieve the highest hemispherical solar distillers performance. Three hemispherical solar distillers of identical dimensions are designed and built, and tested at the same El Oued, Algeria weather conditions, namely; the first is a conventional hemispherical distiller (CHD) that represent the reference case, and the second and third are hemispherical distillers that include contiguous extended cylindrical iron bars (HD-CECIB) at different diameters of (8, 10, 12, and 14 mm). Fig. 1 shows a schematic test rig for a conventional hemispheric solar distiller. The contiguous extended cylindrical iron bars are not present in the first conventional hemispherical solar distiller. In contrast, the contiguous extended cylindrical iron bars of various diameters are present in the other two hemispherical distillers. A round basin, a glass cover, a distillate water tank, and a support framework make up the hemispheric distiller.

All the outer covers of the basins were built of wood, 35 mm thick, with a diameter of 380 mm, 0.1 m^2 effective areas, and a height of 40 mm on the sides. To improve the absorption of sunlight, the basins are coated with black silicon. The dimensions of each distiller cover unit are 400 mm in diameter and 3 mm thick.

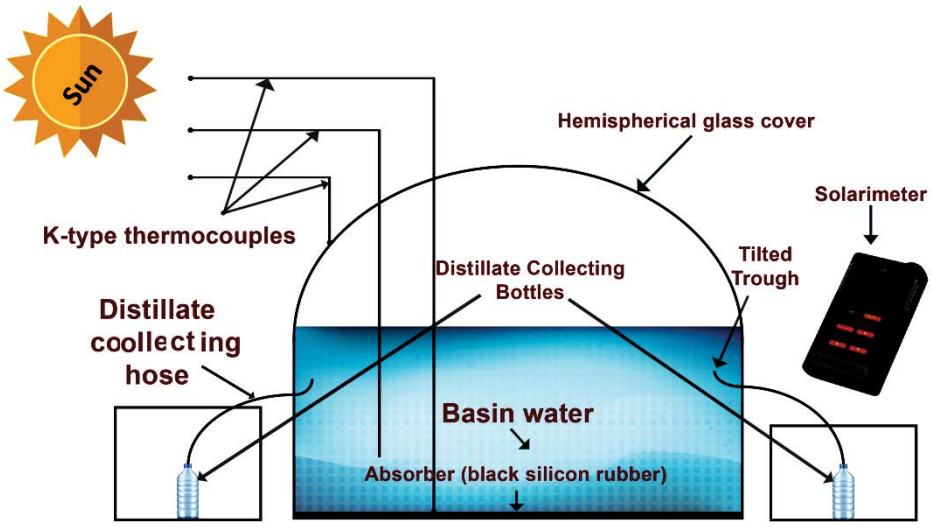

Fig. 1. View of the conventional hemispherical distiller.

Fig. 2 shows the photograph of the cylindrical iron bars with varying diameters of (8, 10, 12, and 14 mm). The experimental installations of the basin of hemispherical solar distillers with extended cylindrical iron bars are shown in Fig. 3. The contiguous extended cylindrical iron bars with varying diameters of (8, 10, 12, and 14 mm) were carefully positioned on the underside of the circular troughs of the hemispherical solar distillers and immersed beneath 2 liters of tap seawater. As shown, Fig. 3 shows the photographic view of the circular basin for the four different test cases of the hemispherical solar distiller with extended cylindrical iron bars, namely; hemispherical distiller with contiguous extended cylindrical iron bars 8 mm diameter (HD-CECIB8), hemispherical distiller with contiguous extended cylindrical iron bars 10 mm diameter (HD-CECIB10), hemispherical distiller with contiguous extended cylindrical iron bars 12 mm diameter (HD-CECIB12), and hemispherical distiller with contiguous extended cylindrical iron bars 14 mm diameter (HD-CECIB14).

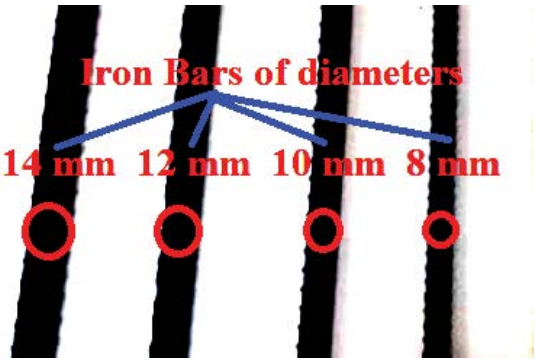

Fig. 2. A photograph of the cylindrical iron bars with varying diameters of (8, 10, 12, and 14 mm).

The thermophysical properties of the iron employed in experimental work are presented in Table 1. All contiguous extended cylindrical iron bars are coated black to improve the intensity of the solar ray's absorption. Fig. 4 shows the photographic view of three hemispherical distillers utilized in the present experimentations test work.

2.2. Instrumentations and uncertainties

The experimentations are conducted in two test scenarios under the same El Oued, Algeria weather conditions to achieve the influences of contiguous extended cylindrical

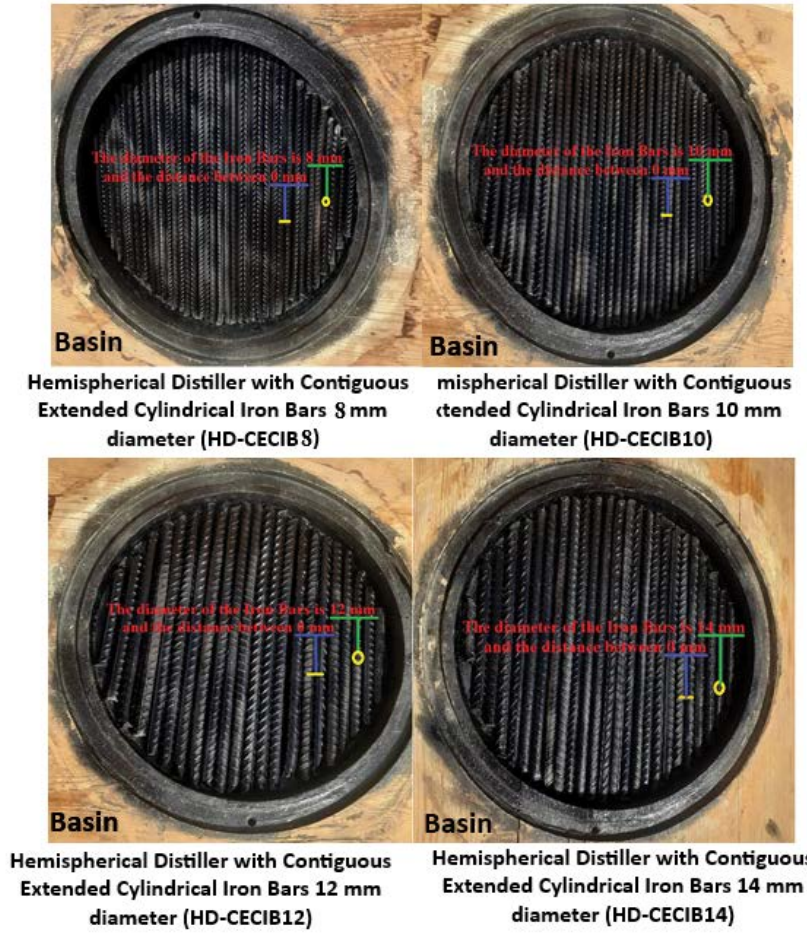

Fig. 3. A photograph of the basin configurations of the hemispherical distillers with contiguous extended cylindrical iron bars with varying diameters of (8, 10, 12, and 14 mm).

iron bars on the performance of the hemispherical solar distiller. Similarly, the optimal diameter of contiguous extended cylindrical iron bars that achieves the highest hemispherical solar distillers performance is also assessed. In the first test scenario, contiguous extended cylindrical iron bars with 8 and 10 mm diameters were installed in second and third distillers (HD-CECIB8 and HD-CECIB10), respectively, and compared to CHD under the same El Oued, Algeria weather conditions. In the second-test scenario, contiguous extended cylindrical iron bars with diameters of 12 and 14 mm were installed in the second and third distillers (HD-CECIB12 and HD-CECIB14), respectively, and compared to CHD under the same El Oued, Algeria weather conditions. In this study, the amount of saltwater within the basin of CHD, HD-CECIB8, HD-CECIB10, HD-CECIB12, and HD-CECIB14 was stable at 2 L for the test periods from 7:00 a.m. to 7:00 p.m. Sunlight radiation, temperatures (basin saltwater, iron bars, cover tube, and ambient air), and collected freshwater were recorded from 7:00 a.m. to 7:00 p.m. during September 2021. The experimental devices were used to measure both temperatures by thermocouples, incident sun rays by a solar power meter, and distillate water by a graduated vessel. Table 2 presents the range, accuracy, and uncertainty of measuring devices used in the present work. Based on the experimental devices' uncertainty, range, and accuracy depicted in Table 2. The relative errors in the overall freshwater production and daily energetic efficiency are computed using the analysis described by Holman [43]. By assuming $uc(y)$ is the total uncertainty of the index y, and y is an experimental value which is a function in individual measurements x_1, $y = f(x_1, x_2, x_3, \ldots, x_n)$. The uncertainty in the measurement results was calculated by [43]:

$$\mathrm{uc}(y) = \sqrt{\sum_{i=1}^{n}\left(\frac{\partial y}{\partial x_i}\right)^2 u^2(x_i)} \tag{1}$$

According to the measurement results and instrument uncertainty, the uncertainty of the overall freshwater production, daily energetic efficiency, and daily exergetic efficiency are 1.92%, 2.86%, and 2.38%, respectively.

Table 1
Thermophysical properties of iron

Properties	Value
Melting temperature, °C	2,082
Latent heat of fusion, kJ/kg	277.4
Thermal conductivity, W/m·K	37.65
Specific heat, kJ/kg·K	0.82
Density, kg/m^3	7,650

3. System performance

The daily thermal efficiency of the distillers $\eta_{daily,th}$, is a vital parameter to figure out the actual improvement in the hemispherical solar distiller performance from the

Table 2
Accuracy and uncertainty values for measurement devices

Device	Accuracy	Range	Uncertainty
Solarimeter	±10 W/m^2	0–1,999 W/m^2	5.78 W/m^2
Thermocouples (K-type)	±0.1°C	−100 – 500°C	0.08°C
Scaled vessel	±1 mL	0–500 mL	0.5 mL

Fig. 4. A photograph of the experimental set-up.

perspective of the total energy received by the distiller. It accounts for the entirety of the hourly yield $\sum \dot{m}_w$, latent heat of the vaporization h_{fg}, daily solar intensity $\sum I(t)$, and basin surface area A_s, as described in the following equation;

$$\eta_{daily,th} = \frac{\sum \dot{m}_w \times h_{fg}}{\sum A_s \times I(t) \times 3{,}600} \quad (2)$$

The daily exergy efficiency $\eta_{daily,exe}$ calculated as follows [44]:

$$\eta_{daily,exe} = \frac{\sum Ex_{output}}{\sum Ex_{input}} \times 100;(\%) \quad (3)$$

The output exergy energy Ex_{output} calculated as [44];

$$Ex_{output} = \frac{\dot{m}_w h_{fg}}{3{,}600}\left[1 - \frac{T_a + 273}{T_w + 273}\right];(W) \quad (4)$$

The input exergy energy (Ex_{input}) calculated as [44];

$$Ex_{input} = A_{ab} I(t)\left[1 - \frac{4}{3}\left(\frac{T_a + 273}{6{,}000}\right) + \frac{1}{3}\left(\frac{T_a + 273}{6{,}000}\right)^4\right];(W) \quad (5)$$

where T_a is a temperature of ambient air (°C) and T_w is water temperature (°C).

The latent heat of the vaporization h_{fg} is calculated as [38]:

$$h_{fg} = 10^3\left[\begin{array}{c} 2501.9 - 2.40706T_w + 1.192217 \times 10^{-3} T_w^2 \\ -1.5863 \times 10^{-5} T_w^3 \end{array}\right] \quad (6)$$

4. Results and discussions

The experimentations were carried out in the Physics Department of the Science Faculty at the University of El Oued in Algeria in September 2021. The data was taken for a period of 12 h, from 7:00 a.m. to 7:00 p.m.

The solar intensity and ambient temperature greatly influence solar distiller performance. As a result, solar ray's intensity and ambient temperature during the experimentations were monitored and recorded during the test days. Fig. 5 displays hourly fluctuation in solar rays and ambient temperatures during the trial hours. The solar ray's intensity on the two test days is nearly identical, which increases until it reaches the maximum intensity of 1,002 W/m² at midday, then gradually decreases as time passes until it reaches its lowest point near sunset. The greatest recorded ambient temperature was also achieved around 3:00 p.m varying between 36°C–50°C and 35°C–50°C on 13-09-2021 and 14-09-2021, respectively. This means that all of the cases may be compared because they are all subjected to the same climatic condition, allowing for more precise comparison.

To get the optimal diameter of contiguous extended cylindrical iron bars that achieves the highest hemispherical distillers performance, the performance of hemispherical distillers with adjacent contiguous extended cylindrical iron bars with diameters of 8, 10, 12, and 14 mm (HD-CECIB8, HD-CECIB10, HD-CECIB12, and HD-CECIB14) is compared to that of the conventional hemispherical distiller under the identical conditions (CHD).

Fig. 6 displays the hourly change in water basin temperature for five distinct configurations of the hemispherical solar distillers from 7:00 a.m.–7:00 p.m. The hourly temperature variation appears to increase as the diameter of contiguous extended cylindrical iron bars increases. The maximum water basin temperature of the CHD, HD-CECIB8, HD-CECIB10, HD-CECIB12 and HD-CECIB14 reaches 65°C, 69°C, 72°C, 75°C, and 78°C, respectively, at about 2:00 p.m. It is noted that during the period from 7:00 a.m.–7:00 p.m., the use of contiguous extended cylindrical iron bars is very effective, which causes to rises the basin water temperatures throughout compared to the CHD. The maximum improvement in basin water temperature was recorded when using contiguous extended cylindrical iron bars with a diameter of 14 mm (HD-CECIB14); therefore, this diameter represents the best diameter that achieves the highest hemispherical solar distillers performance. This is due to the increase in the surface area of absorption of solar

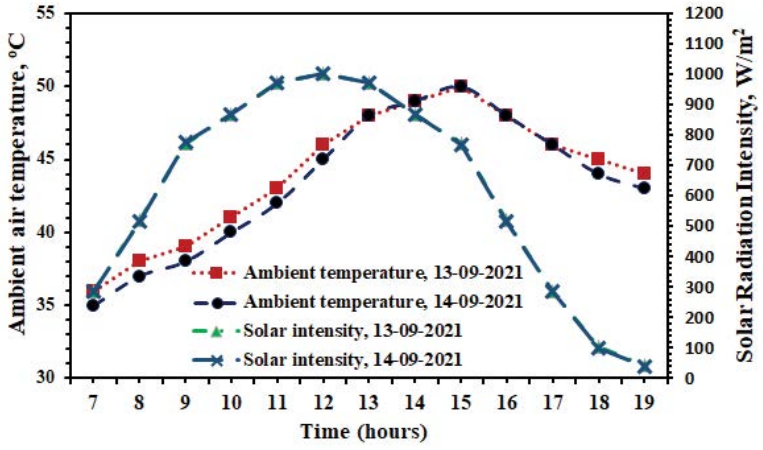

Fig. 5. Hourly variations of solar rays and ambient temperature with daytime.

radiation because the absorber surface after installing the contiguous extended cylindrical iron bars is characterized as similar to the semi-circular corrugated surface, improving the thermal properties of the absorber surface, in addition to the extended cylindrical iron bars as sensible storage materials.

The temperature differences between the trays of water and outside of the glass cover are a substantial indicator of the condensation rates of the water vapor generated inside the hemispherical distillers and then a substantial indicator of distiller productivity. Fig. 7 depicts the temperature difference between the trays of water and the outside of the glass cover for CHD, HD-CECIB8, HD-CECIB10, HD-CECIB12, and HD-CECIB14. As shown, the maximum temperature difference between the tray water and outside reached 6°C, while the use of contiguous extended cylindrical iron bars will cause a rise in the maximum temperature difference to 11°C, 14°C, 17°C, and 19°C for cylindrical iron bars diameters of 8, 10, 12, and 14 mm, respectively. This figure depicts that the maximum improvement in the temperature difference between trays water and outside was recorded when using contiguous extended cylindrical iron bars with a diameter of 14 mm (HD-CECIB14), and therefore this diameter represents the best diameter that achieves the highest hemispherical solar distillers performance.

Contiguous extended cylindrical iron bar diameters influence the hourly productivity of hemispherical distillers. Fig. 8 addresses the hourly change in distillate yield for the various configurations of hemispherical distillers (CHD, HD-CECIB8, HD-CECIB10, HD-CECIB12, and HD-CECIB14) from 7:00 a.m. – 7:00 p.m. As presented, the hourly variance of the collected freshwater production of the hemispherical distiller increases with the increase in the diameter of cylindrical iron bars. As a result, the maximum hourly collected distillate water production of various configurations of hemispherical distillers reaches 0.8, 1.1, 1.15, 1.22, and 1.3 L/m^2-h for CHD, HD-CECIB8, HD-CECIB10, HD-CECIB12, and HD-CECIB14, respectively. The results of hourly collected distillate water production indicated that the utilization of the contiguous extended cylindrical iron bars with a diameter of 14 mm (HD-CECIB14) represents the optimal diameter that achieves the highest accumulative distillate water production.

Fig. 9 depicts the influence of contiguous extended cylindrical iron bars diameters on the accumulative distillate productivity of hemispherical solar distillers. As presented, the

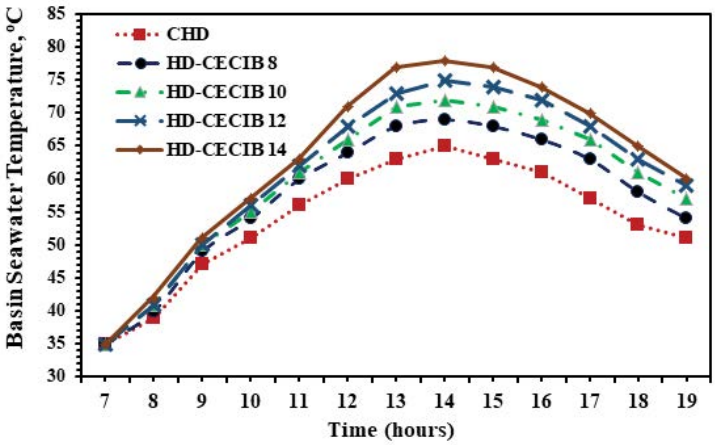

Fig. 6. Variations of the water basin temperature with daytime for different diameters of cylindrical iron bars.

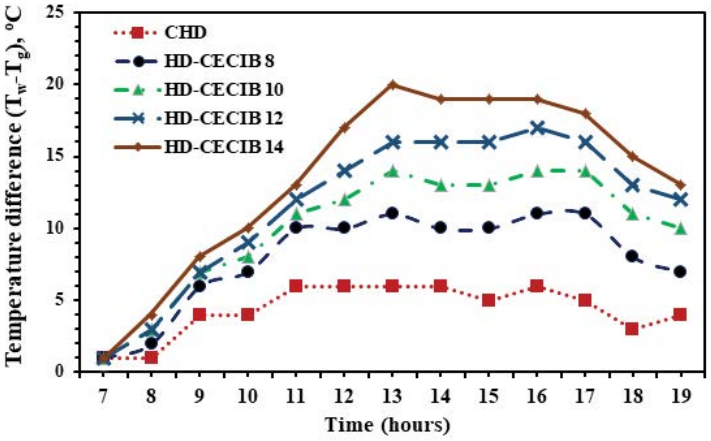

Fig. 7. Hourly variation of the temperature difference with daytime for different diameters of cylindrical iron bars.

accumulative distillate productivity increases with increasing the diameter of contiguous extended cylindrical iron bars. As a result, the cumulative collected distillate water production of various configurations of hemispherical distillers reaches 4.8, 6.95, 7.4, 7.91, and 8.35 L/m^2·d for CHD, HD-CECIB8, HD-CECIB10, HD-CECIB12, and HD-CECIB14, respectively. These findings indicated that utilization of the contiguous extended cylindrical iron bars represents the most effective choice to improve cumulative distillate water production. The cumulative distillate water production improvement rates for utilizing the contiguous extended cylindrical iron bars reach 44.8%, 54.2%, 64.8%, and 74% for HD-CECIB8, HD-CECIB10, HD-CECIB12, and HD-CECIB14, respectively compared to CHD (Fig. 10). These results indicated that the utilization of the contiguous extended cylindrical iron bars with a diameter of 14 mm (HD-CECIB14) represents the optimal diameter that achieves the highest accumulative distillate water production.

Fig. 11 illustrates the influences of contiguous extended cylindrical iron bars diameters on the daily thermal efficiency of hemispherical solar distillers. As presented, the daily thermal efficiency increases with increasing the contiguous extended cylindrical iron bar diameters. The daily thermal efficiency of various configurations of hemispherical distillers reaches 40.8%, 58.9%, 62.6%, 66.8%, and 70.3% for CHD, HD-CECIB8, HD-CECIB10, HD-CECIB12, and HD-CECIB14, respectively. These findings indicated that utilization of the contiguous extended cylindrical iron bars represents the most effective choice to improve the performance of hemispherical solar distillers. Also, as shown in Fig. 11, improvement rates in the daily thermal efficiency for using the contiguous extended cylindrical iron bars reach 44.4%, 53.4%, 63.7%, and 72.3% at bars diameters of 8, 10, 12, and 14 mm (HD-CECIB8, HD-CECIB10, HD-CECIB12, and HD-CECIB14), respectively compared to CHD. These results indicated that the utilization of the contiguous extended cylindrical iron bars with a diameter of 14 mm (HD-CECIB14) represents the optimal diameter that achieves the highest hemispherical solar distillers performance.

Fig. 12 illustrates the influences of contiguous extended cylindrical iron bars diameters on the daily exergy efficiency of hemispherical solar distillers. The daily exergy efficiency of various configurations of hemispherical distillers reaches 1.67%, 3.23%, 3.78%, 4.58%, and 5.17% for CHD, HD-CECIB8, HD-CECIB10, HD-CECIB12, and HD-CECIB14, respectively. These results presented that the

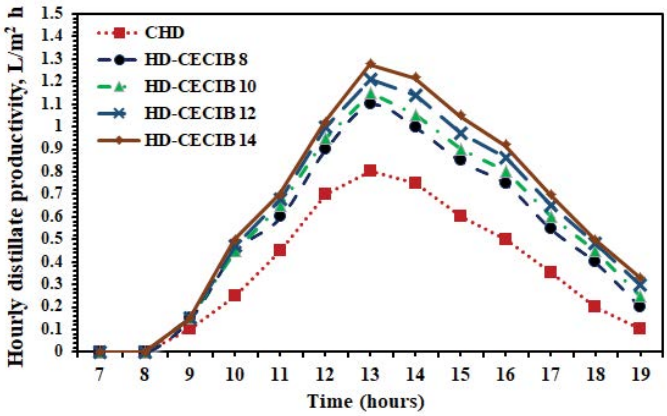

Fig. 8. Variation of the hourly collected distillate water production with daytime for different diameters of cylindrical iron bars.

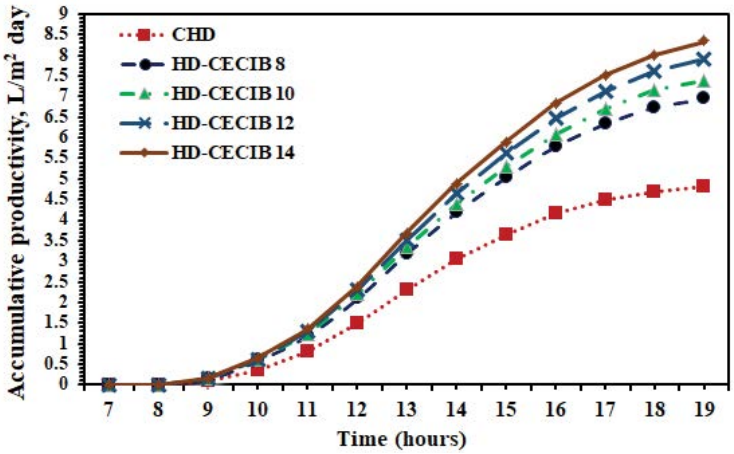

Fig. 9. Cumulative collected distillate water production with daytime for different diameters of cylindrical iron bars.

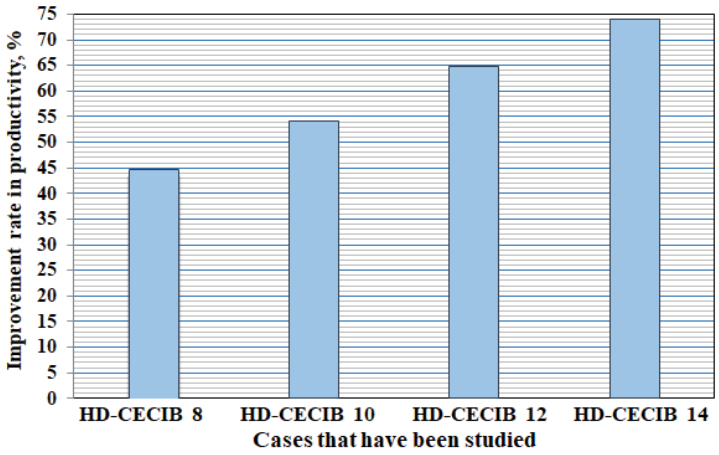

Fig. 10. Improvement rates in cumulative production for various configurations of hemispherical distillers with cylindrical iron bars.

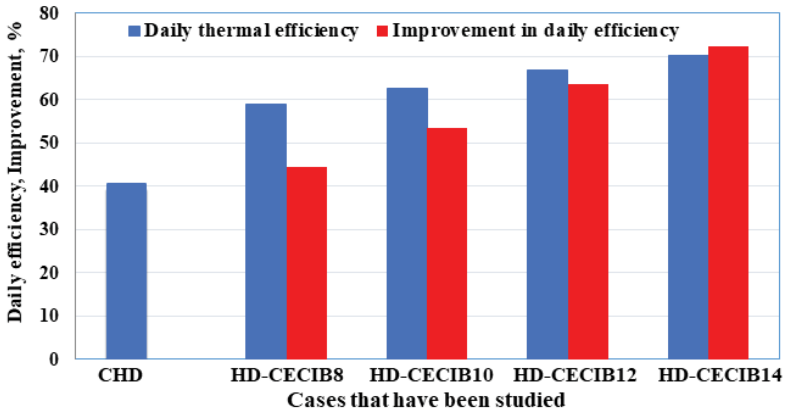

Fig. 11. Thermal efficiency of hemispherical distillers with different diameters of cylindrical iron bars.

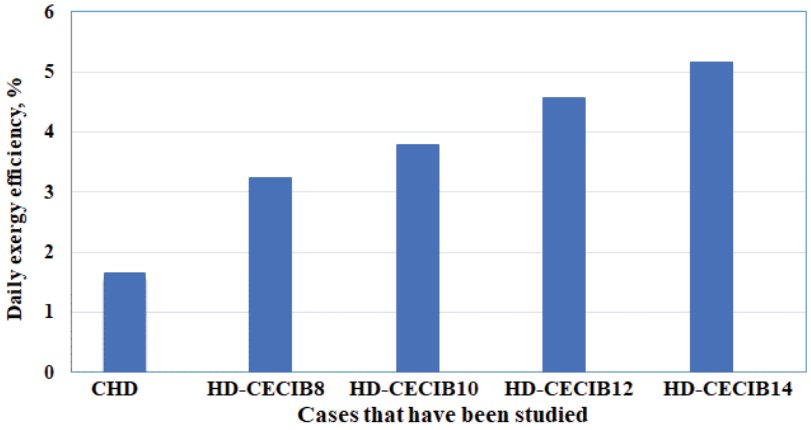

Fig. 12. Exergy efficiency of hemispherical distillers with different diameters of cylindrical iron bars.

daily exergy efficiency increases with increasing the contiguous extended cylindrical iron bar diameters. Also, the maximum improvement in exergy efficiency reached 209.6% for utilizing the contiguous extended cylindrical iron bars with a diameter of 14 mm (HD-CECIB14).

5. Comparison of the current study with similar published works

To clarify the significance of utilizing a proposed contiguous extended cylindrical iron bars in the present

Table 3
Accumulated yield enhancement of the present and previous works

Author(s) and reference	Design of solar distillers	Absorbers used	Productivity increase (%)
Rattanpol et al. [45]	Single slope	- Fins	20.00
Attia et al. [46]	Single slope	- Aluminum balls	37.19
Attia et al. [47]	Hemispherical	- Layer of phosphate pellets	37.40
		- 10 g/L of phosphate pellets	33.70
		- 20 g/L of phosphate pellets	47.90
Attia et al. [48]	Hemispherical	- Tray of iron	14.60
		- Tray of zinc	31.25
		- Tray of copper	53.12
Ouar et al. [49]	Single slope	- Bitumen-charcoal – black ink	18.32
Haddad et al. [50]	Single slope	- Wick	14.72
Elango and Murugavel [51]	Double slope	- Black coating	17.38
Present work	Hemispherical	- Contiguous cylindrical iron bars (8 mm diameter)	44.8
		- Contiguous cylindrical iron bars (10 mm diameter)	54.2
		- Contiguous cylindrical iron bars (12 mm diameter)	64.8
		- Contiguous cylindrical iron bars (14 mm diameter)	74

Table 4
Fabrication cost of CHD, HD-CECIB8, HD-CECIB10, HD-CECIB12, and HD-CECIB14

	CHD	HD-CECIB8	HD-CECIB10	HD-CECIB12	HD-CECIB14
Total capital cost, ($)	67.78	68.53	68.68	68.83	68.98
Annual fixed cost, ($)	11.98	12.13	12.16	12.18	12.21
Annual operating and maintenance cost, ($)	3.59	3.64	3.65	3.66	3.67
Annual salvage, ($)	0.77	0.78	0.783	0.784	0.786
Annual total cost, ($)	14.8	14.99	15.03	15.06	15.1
Annual productivity, (L/m^2·y)	1,296	1,877	1,998	2,136	2,255
Freshwater production cost per liter, ($/L)	0.0114	0.008	0.0075	0.0071	0.0067

experimentations to ameliorate the performance of hemispherical solar distillers. A comparison between the results of our experimentations for various configurations of hemispherical solar distillers with contiguous extended cylindrical iron bars and these of other relevant studies established in solar distillers has been demonstrated in Table 3. The obtained enhancements in the cumulative water production exhibited good performance for the hemispherical solar distillers with contiguous extended cylindrical iron bars with a diameter of 14 mm (HD-CECIB14) compared to those revealed by other previous works.

6. Economic evaluation

In this section, a comprehensive economic study was conducted to assess the economic feasibility of the developed modifications applied to the hemispherical solar distiller's configurations, to calculate and compare the distillate water cost per liter ware produced from the various configurations of the hemispherical distillers suggested in this study. The economic feasibility study was completed based on the calculation method described by [4,13]. Table 4 demonstrates the results of the comprehensive economic analysis of the various configurations of the hemispherical distillers suggested in this study. The economic findings revealed that the utilization of contiguous extended cylindrical iron bars reduced the freshwater cost per liter by 29.8%, 34.2%, 37.7%, and 41.2% for HD-CECIB8, HD-CECIB10, HD-CECIB12, and HD-CECIB14, respectively, compared to the reference distiller (CHD).

7. Conclusions

An experimental investigation was carried out in order to enhance the performance of a hemispherical solar distiller by using contiguous extended cylindrical iron bars as energy storage corrugated absorbers. After installing the contiguous extended cylindrical iron bars, the absorber surface is similar to the semi-circular corrugated surface, in addition to the extended cylindrical iron bars representing sensible storage materials. To get the optimal diameter of contiguous extended cylindrical iron bars that achieve the highest performance, three distillers were designed, fabricated, and tested in the same El Oued, Algeria weather conditions, namely; conventional hemispherical distiller (CHD), which represent a reference case, and second and third are

hemispherical distillers that include contiguous extended cylindrical iron bars (HD-CECIB) at different diameters of 8, 10, 12, and 14 mm. The following are the significant findings:

- The yield of a hemispherical distiller with contiguous extended cylindrical iron bars reaches 6.95, 7.4, 7.91, and 8.35 L/m^2·d for HD-CECIB8, HD-CECIB10, HD-CECIB12, and HD-CECIB14, respectively, compared to 4.8 L/m^2·d that achieved by reference distiller (CHD).
- The improvement in yield of the hemispherical distillers for using contiguous extended cylindrical iron bars reached 44.8%, 54.2%, 64.8%, and 74% for HD-CECIB8, HD-CECIB10, HD-CECIB12, and HD-CECIB14, respectively compared to CHD.
- The improvement rates in daily thermal efficiency for utilizing contiguous extended cylindrical iron bars reach 44.4%, 53.4%, 63.7%, and 72.3% for HD-CECIB8, HD-CECIB10, HD-CECIB12, and HD-CECIB14, respectively compared to CHD.
- The economic findings revealed that the utilization of contiguous extended cylindrical iron bars reduced the freshwater cost per liter by 29.8%, 34.2%, 37.7%, and 41.2% for HD-CECIB8, HD-CECIB10, HD-CECIB12, and HD-CECIB14, respectively, compared to reference distiller (CHD).
- The utilization of contiguous extended cylindrical iron bars with a diameter of 14 mm (HD-CECIB14) represents the optimal diameter that achieves the highest hemispherical solar distiller performance.

Finally, employing cylindrical iron bars as extended fins to boost distillation yield is an excellent, easy, and simple suggestion that should be used.

Abbreviations

PCM	—	Phase change materials
SS	—	Solar still
CHD	—	Conventional hemispherical distiller
HD-CECIB8	—	Hemispherical distiller with contiguous extended cylindrical iron bars 8 mm diameter
HD-CECIB10	—	Hemispherical distiller with contiguous extended cylindrical iron bars 10 mm diameter
HD-CECIB12	—	Hemispherical distiller with contiguous extended cylindrical iron bars 12 mm diameter
HD-CECIB14	—	Hemispherical distiller with contiguous extended cylindrical iron bars 14 mm diameter

References

[1] M. Appadurai, V. Velmurugan, Performance analysis of fin type solar still integrated with fin type mini solar pond, Sustainable Energy Technol. Assess., 9 (2015) 30–36.
[2] M.E.H. Attia, Z. Driss, A.E. Kabeel, M. Abdelgaied, A.M. Manokar, R. Sathyamurthy, A.K. Hussein, Performance evaluation of modified solar still using aluminum foil sheet as absorber cover – a comparative study, J. Test. Eval., 49 (2021), doi: 10.1520/JTE20200249.
[3] A.E. Kabeel, M. Abdelgaied, K. Harby, A. Eisa, Augmentation of diurnal and nocturnal distillate of modified tubular solar still having copper tubes filled with PCM in the basin, J. Energy Storage, 32 (2020) 101992, doi: 10.1016/j.est.2020.101992.
[4] A.E. Kabeel, M. Abdelgaied, Solar energy assisted desiccant air conditioning system with PCM as a thermal storage medium, Renewable Energy, 122 (2018) 632–642.
[5] A.E. Kabeel, M. Abdelgaied, Performance of novel solar dryer, Process Saf. Environ. Prot., 102 (2016) 183–189.
[6] F.A. Essa, Z. Omara, A. Abdullah, S. Shanmugan, H. Panchal, A.E. Kabeel, R. Sathyamurthy, M.M. Athikesavan, A. Elsheikh, M. Abdelgaied, B. Saleh, Augmenting the productivity of stepped distiller by corrugated and curved liners, CuO/paraffin wax, wick, and vapor suctioning, Environ. Sci. Pollut. Res., 28 (2021) 56955–56965.
[7] S. Shoeibi, N. Rahbar, A.A. Esfahlani, H. Kargarsharifabad, Improving the thermoelectric solar still performance by using nanofluids – experimental study, thermodynamic modeling and energy matrices analysis, Sustainable Energy Technol. Assess., 47 (2021) 101339, doi: 10.1016/j.seta.2021.101339.
[8] A.E. Kabeel, M. Abdelgaied, Observational study of modified solar still coupled with oil serpentine loop from cylindrical parabolic concentrator and phase changing material under basin, Sol. Energy, 144 (2017) 71–78.
[9] S. Shoeibi, H. Kargarsharifabad, N. Rahbar, G. Ahmadi, M.R. Safaei, Performance evaluation of a solar still using hybrid nanofluid glass cooling-CFD simulation and environmental analysis, Sustainable Energy Technol. Assess., 49 (2022) 101728, doi: 10.1016/j.seta.2021.101728.
[10] S.K. Singh, S.C. Kaushik, V.V. Tyagi, S.K. Tyagi, Comparative performance and parametric study of solar still: a review, Sustainable Energy Technol. Assess., 47 (2021) 101541, doi: 10.1016/j.seta.2021.101541.
[11] P. Pal, S.K. Patel, A. Bharti, A. Narayan, R. Dev, D. Singh, Energy, exergy, energy matrices, exergoeconomic and enviroeconomic assessment of modified solar stills, Sustainable Energy Technol. Assess., 47 (2021) 101514, doi: 10.1016/j.seta.2021.101514.
[12] A.E. Kabeel, M. Abdelgaied, A. Eisa, Enhancing the performance of single basin solar still using high thermal conductivity sensible storage materials, J. Cleaner Prod., 183 (2018) 20–25.
[13] M.E.H. Attia, A.E. Kabeel, M. Abdelgaied, G.B. Abdelaziz, A comparative study of the effect of internal reflectors on a performance of hemispherical solar distillers: Energy, exergy, and economic analysis, Sustainable Energy Technol. Assess., 47 (2021) 101465, doi: 10.1016/j.seta.2021.101465.
[14] A. Bellila, M.E.H. Attia, A.E. Kabeel, M. Abdelgaied, K. Harby, J. Soli, Productivity enhancement of hemispherical solar still using Al_2O_3-water based nanofluid and cooling the glass cover, Appl. Nanosci., 11 (2021) 1127–1139.
[15] A.K. Thakur, R. Sathyamurthy, S.W. Sharshir, A.E. Kabeel, M.R. Elkadeem, Z. Ma, A.M. Manokar, M. Arıcı, A.K. Pandey, R. Saidur, Performance analysis of a modified solar still using reduced graphene oxide coated absorber plate with activated carbon pellet, Sustainable Energy Technol. Assess., 45 (2021) 101046, doi: 10.1016/j.seta.2021.101046.
[16] M.E.H. Attia, A.E. Kabeel, M. Abdelgaied, A. Bellila, M.M. Abdel-Aziz, Optimal concentration of high thermal conductivity sensible storage materials (graphite) for performance enhancement of hemispherical distillers, Desal. Water Treat., 231 (2021) 263–272.
[17] M.E.H. Attia, A.E. Kabeel, M. Abdelgaied, A. Bellila, M.M. Abdel-Aziz, A. Abdullah, Optimal size of black gravel as energy storage materials for performance improvement of hemispherical distillers, J. Energy Storage, 43 (2021) 103196, doi: 10.1016/j.est.2021.103196.
[18] M.E.H. Attia, A.E. Kabeel, M. Abdelgaied, Optimal concentration of El Oued sand grains as energy storage materials for enhancement of hemispherical distillers performance, J. Energy Storage, 36 (2021) 102415, doi: 10.1016/j.est.2021.102415.
[19] M.E.H. Attia, Z. Driss, A.E. Kabeel, K. Alagar, M.M. Athikesavan, R. Sathyamurthy, Phosphate bags as energy storage materials for enhancement of solar still performance, Environ. Sci. Pollut. Res. Int., 28 (2021) 21540–21552.

[20] M.E.H. Attia, A.E. Kabeel, M. Abdelgaied, Z. Driss, Productivity enhancement of traditional solar still by using sandbags of El Oued (Algeria), Heat Transfer, 50 (2021) 768–783.
[21] H. Panchal, P. Patel, N. Patel, H. Thakkar, Performance analysis of solar still with different energy-absorbing materials, Int. J. Ambient Energy, 38 (2017) 224–228.
[22] B. Nasri, A. Benatiallah, S. Kalloum, D. Benatiallah, Improvement of glass solar still performance using locally available materials in the southern region of Algeria, Groundwater Sustainable Dev., 9 (2019) 100213, doi: 10.1016/j.gsd.2019.100213.
[23] M. Abdelgaied, K. Harby, A. Eisa, Experimental investigation on the performance improvement of tubular solar still using floating black sponge layer, Environ. Sci. Pollut. Res., 28 (2021) 34968–34978.
[24] B. Madhu, E. Balasubramanian, R. Sathyamurthy, P.K. Nagarajan, D. Mageshbabu, R. Bharathwaaj, A.M. Manokar, Exergy analysis of solar still with sand heat energy storage, Appl. Sol. Energy, 54 (2018) 173–177.
[25] A.E. Kabeel, E.S. El-Agouz, M.M. Athikesavan, R.D. Ramalingam, R. Sathyamurthy, N. Prakash, C. Prasad, Comparative analysis on freshwater yield from conventional basin-type single slope solar still with cement-coated red bricks: an experimental approach, Environ. Sci. Pollut. Res., 27 (2020) 32218–32228.
[26] M.E.H. Attia, A.E. Kabeel, M. Abdelgaied, W.M. El-Maghlany, A. Bellila, Comparative study of hemispherical solar distillers iron-fins, J. Cleaner Prod., 292 (2021) 126071, doi: 10.1016/j.jclepro.2021.126071.
[27] G.B. Balachandran, P.W. David, G. Rajendran, M.N.A. Ali, V. Radhakrishnan, R. Balamurugan, M.M. Athikesavan, R. Sathyamurthy, Investigation of performance enhancement of solar still incorporated with *Gallus gallus domesticus* cascara as sensible heat storage material, Environ. Sci. Pollut. Res., 28 (2021) 611–624.
[28] M. Abdelgaied, Y. Zakaria, A.E. Kabeel, F.A. Essa, Improving the tubular solar still performance using square and circular hollow fins with phase change materials, J. Energy Storage, 38 (2021) 102564, doi: 10.1016/j.est.2021.102564.
[29] R. Sathyamurthy, D. Mageshbabu, B. Madhu, A.M. Manokar, A.R. Prasad, M. Sudhakar, Influence of fins on the absorber plate of tubular solar still – an experimental study, Mater. Today:. Proc., 46 (2021) 3270–3274.
[30] J. Kateshia, V.J. Lakhera, Analysis of solar still integrated with phase change material and pin fins as absorbing material, J. Energy Storage, 35 (2021) 102292, doi: 10.1016/j.est.2021.102292.
[31] K.M. Bataineh, M.A. Abbas, Performance analysis of solar still integrated with internal reflectors and fins, Sol. Energy, 205 (2020) 22–36.
[32] A.F. Mohamed, A.A. Hegazi, G.I. Sultan, E.M.S. El-Said, Enhancement of a solar still performance by inclusion the basalt stones as a porous sensible absorber: experimental study and thermo-economic analysis, Sol. Energy Mater. Sol. Cells, 200 (2019) 109958, doi: 10.1016/j.solmat.2019.109958.
[33] A.E. Kabeel, G.B. Abdelaziz, E.M.S. El-Said, Experimental investigation of a solar still with composite material heat storage: energy, exergy and economic analysis, J. Cleaner Prod., 231 (2019) 21–34.
[34] A.E. Kabeel, E.M.S. El-Said, Experimental study on a modified solar power driven hybrid desalination system, Desalination, 443 (2018) 1–10.
[35] A.E. Kabeel, T.A. Elmaaty, E.M.S. El-Said, Economic analysis of a small-scale hybrid air HDH–SSF (humidification and dehumidification–water flashing evaporation) desalination plant, Energy, 53 (2013) 306–311.
[36] A.E. Kabeel, M. Abdelgaied, M.B. Feddaoui, Hybrid system of an indirect evaporative air cooler and HDH desalination system assisted by solar energy for remote areas, Desalination, 439 (2018) 162–167.
[37] A.E. Kabeel, M. Abdelgaied, R. Sathyamurthy, A comprehensive investigation of the optimization cooling technique for improving the performance of PV module with reflectors under Egyptian conditions, Sol. Energy, 186 (2019) 257–263.
[38] A.E. Kabeel, M.M. Bassuoni, M. Abdelgaied, Experimental study of a novel integrated system of indirect evaporative cooler with internal baffles and evaporative condenser, Energy Convers. Manage., 138 (2017) 518–525.
[39] A.M. Elzahzby, A.E. Kabeel, M.M. Bassuoni, M. Abdelgaied, Effect of inter-cooling on the performance and economics of a solar energy assisted hybrid air conditioning system with six stages one-rotor desiccant wheel, Energy Convers. Manage., 78 (2014) 882–896.
[40] A.E. Kabeel, M. Abdelgaied, R. Sathyamurthy, T. Arunkumar, Performance improvement of a hybrid air conditioning system using the indirect evaporative cooler with internal baffles as a pre-cooling unit, Alexandria Eng. J., 56 (2017) 395–403.
[41] A.E. Kabeel, E.M.S. El-Said, Development strategies and solar thermal energy utilization for water desalination systems in remote regions: a review, Desal. Water Treat., 52 (2014) 4053–4070.
[42] M. Abdelgaied, A.E. Kabeel, A.W. Kandeal, H.F. Abosheiasha, S.M. Shalaby, M.H. Hamed, N. Yang, S.W. Sharshir, Performance assessment of solar PV-driven hybrid HDH-RO desalination system integrated with energy recovery units and solar collectors: theoretical approach, Energy Convers. Manage., 239 (2021) 114215, doi: 10.1016/j.enconman.2021.114215.
[43] J.P. Holman, Experimental Methods for Engineers, 8th ed., McGraw-Hill Companies, New York, 2012.
[44] A.M. Manokar, D.P. Winston, A.E. Kabeel, R. Sathyamurthy, Sustainable fresh water and power production by integrating PV panel in inclined solar still, J. Cleaner Prod., 172 (2018) 2711–2719.
[45] P.N.A. Rattanpol, N. Pichal, A. Wirut, The thermal performance of an ethanol solar still with fin plate to increase productivity, Renewable Energy, 54 (2013) 227–234.
[46] M.E.H. Attia, Z. Driss, A.M. Manokar, R. Sathyamurthy, Effect of aluminum balls on the productivity of solar distillate, J. Energy Storage, 30 (2020) 101466, doi: 10.1016/j.est.2020.101466.
[47] M.E.H. Attia, A.E. Kabeel, M. Abdelgaied, W.M. El-Maghlany, Z. Driss, Enhancement of the performance of hemispherical distiller via phosphate pellets as energy storage medium, Environ. Sci. Pollut. Res., 28 (2021) 32386–32395.
[48] M.E.H. Attia, A.E. Kabeel, M. Abdelgaied, F.A. Essa, Enhancement of hemispherical solar still productivity using iron, zinc and copper trays, Sol. Energy, 216 (2021) 295–302.
[49] M.A. Ouar, M.H. Sellami, S.E. Meddour, R. Touahir, S. Guemari, K. Loudiyi, Experimental yield analysis of groundwater solar desalination system using absorbent materials, Groundwater Sustainable Dev., 5 (2017) 261–267.
[50] Z. Haddad, A. Chaker, A. Rahmani, Improving the basin type solar still performances using a vertical rotating wick, Desalination, 418 (2017) 71–78.
[51] T. Elango, K.K. Murugavel, The effect of the water depth on the productivity for single and double basin double slope glass solar stills, Desalination, 359 (2015) 82–91.